AD-A059 883 NAVAL RESEARCH LAB WASHINGTON D C F/G 20/8
DYNAMICS AND RADIATIVE YIELDS FROM ALUMINUM MULTIPLE WIRE ARRAY--ETC(U)
AUG 78 D G COLOMBANT, M LAMPE, J DAVIS

UNCLASSIFIED NRL-MR-3840 NL

| OF |
AD
A059883

END
DATE
FILMED
12-78
DDC

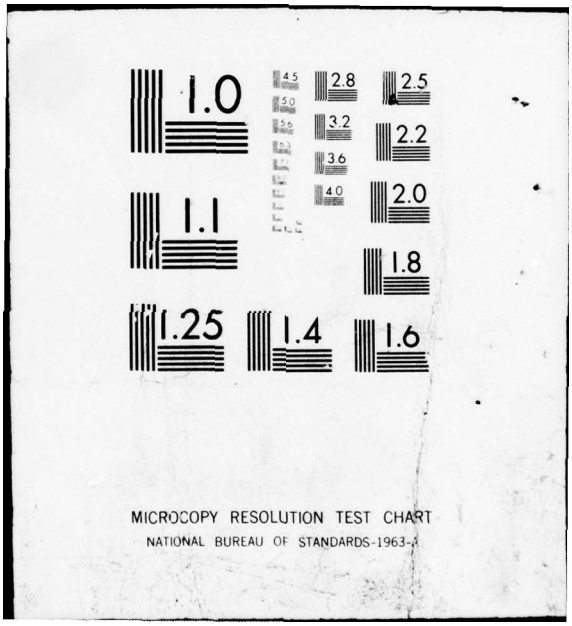
1.0
1.1
1.25
1.4
1.6
1.8
2.0
2.2
2.5
2.8
3.2
3.6
4.0
4.5
5.0
5.6
MICROCOPY RESOLUTION TEST CHART
NATIONAL BUREAU OF STANDARDS-1963-A

NRL Memorandum Report 3840

Dynamics and Radiative Yields from Aluminum Multiple Wire Arrays

D.G. Colombant, M. Lampe, and J. Davis

Plasma Physics Division

and

H.W. Bloomberg

Science Applications, Inc.
McLean, Virginia 22101

August 1978

This research was sponsored by the Defense Nuclear Agency under Subtask T99QAXLB203, work unit 12 and work unit title, Advanced Concepts Theory.

NAVAL RESEARCH LABORATORY
Washington, D.C.

SECURITY CLASSIFICATION OF THIS PAGE (When Data Entered)

REPORT DOCUMENTATION PAGE

READ INSTRUCTIONS BEFORE COMPLETING FORM

1. REPORT NUMBER
NRL Memorandum Report 3840

2. GOVT ACCESSION NO.
NRL-MR

3. RECIPIENT'S CATALOG NUMBER

4. TITLE (and Subtitle)
Dynamics and Radiative Yields from Aluminum Multiple Wire Arrays,

5. TYPE OF REPORT & PERIOD COVERED
Interim report on a continuing NRL Problem

6. PERFORMING ORG. REPORT NUMBER

7. AUTHOR(s)
D. G. Colombant, M. Lampe, J. Davis and H. W. Bloomberg*

8. CONTRACT OR GRANT NUMBER(s)

9. PERFORMING ORGANIZATION NAME AND ADDRESS
Naval Research Laboratory
Washington, D.C. 20375

10. PROGRAM ELEMENT, PROJECT, TASK AREA & WORK UNIT NUMBERS
NRL Problem # H02-26L.

11. CONTROLLING OFFICE NAME AND ADDRESS
Defense Nuclear Agency
Washington, D.C. 20305

12. REPORT DATE
August 1978

13. NUMBER OF PAGES
53

14. MONITORING AGENCY NAME & ADDRESS (if different from Controlling Office)
53 p.

15. SECURITY CLASS. (of this report)
UNCLASSIFIED

15a. DECLASSIFICATION/DOWNGRADING SCHEDULE
UNCLASSIFIED

16. DISTRIBUTION STATEMENT (of this Report)
Approved for public release; distribution unlimited.

17. DISTRIBUTION STATEMENT (of the abstract entered in Block 20, if different from Report)
B203

18. SUPPLEMENTARY NOTES
This research was sponsored by the Defense Nuclear Agency under Subtask T99QAXLB203; Work Unit Code and Title - 12 "Advanced Concepts Theory".
*Science Applications, Inc. McLean, Virginia 22101

19. KEY WORDS (Continue on reverse side if necessary and identify by block number)
Exploding wires, X-ray sources, Z-pinches

20. ABSTRACT (Continue on reverse side if necessary and identify by block number)
Numerical results are presented for the dynamics and radiative yields from aluminum multiple wire arrays. In order to reach qualitative agreement with experimental results, it is found that the introduction of an enhanced anomalous resistivity is required. Physical origin of enhanced resistivity is briefly discussed.

DD FORM 1 JAN 73 1473 EDITION OF 1 NOV 65 IS OBSOLETE
S/N 0102-LF-014-6601

251 950

SECURITY CLASSIFICATION OF THIS PAGE (When Data Entered)

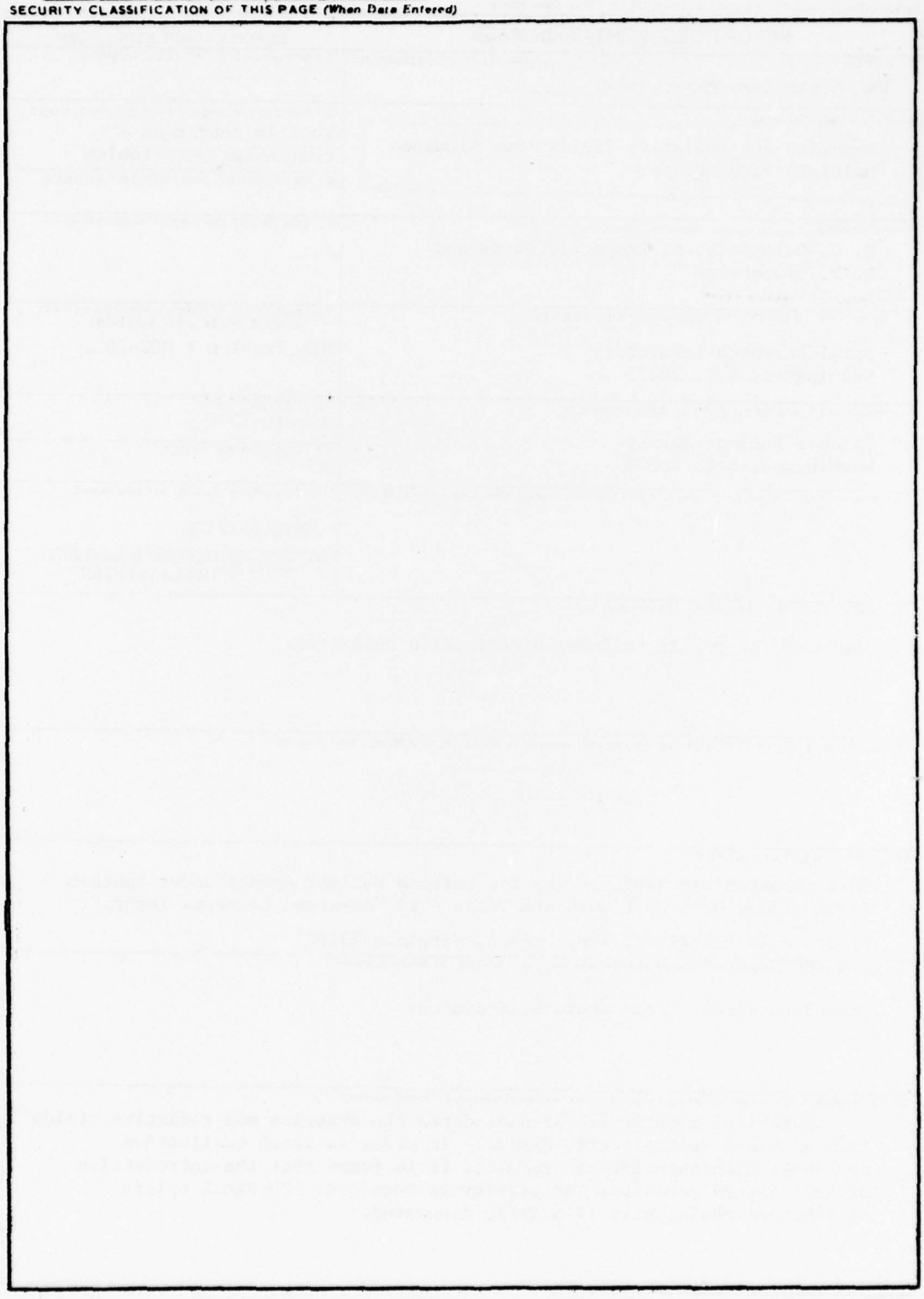

CONTENTS

I.	INTRODUCTION	1
II.	REVIEW OF EXPERIMENTAL RESULTS	3
III.	THEORETICAL CONSIDERATIONS	5
IV.	NUMERICAL STUDIES	12
V.	CONCLUSIONS	19
	REFERENCES	22

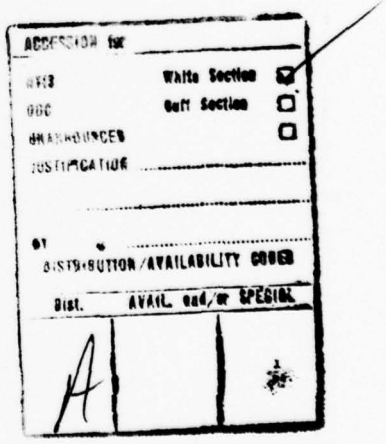

DYNAMICS AND RADIATIVE YIELDS FROM ALUMINUM MULTIPLE WIRE ARRAYS

I. Introduction

In recent years, very impressive progress has been made in the development of multiple exploding wire arrays as x-ray sources using the new high-power generators, Pithon at Physics International (PI) and Blackjack IV at Maxwell Laboratories (MLI). These results also demonstrate the exceedingly complex nature of the physical processes characteristic of exploding wire radiation sources. Axial structure, including sausaging, flared and pinched regions, kinks and hot spots, is clearly seen, and may play an essential role in the radiation emission. Energy coupling from the generator to the wire plasma is sometimes poor. Energy may also be dissipated in field emitted electrons and/or ions, and in radiation-induced plasma short circuits. Non-fluid effects, e.g. runaway electrons, appear to occur in the wire plasma. Azimuthal asymmetries originating in the behavior of the separate wires at early times (i.e. before they assemble) may also play an important role. It appears that a complete theoretical analysis of wire phenomenology will eventually have to come to grips with all of these phenomena - i.e. variation in all three dimensions r, θ, z, as well as non-fluid and diode effects.

These different aspects of multiple wire phenomena are presently under study in our program and elsewhere; azimuthal asymmetries and

Note: Manuscript submitted July 10, 1978.

individual wire effects are discussed in a concurrent report[1], and other aspects of the problem will be reported on subsequently. The present report deals with a further elaboration of the azimuthally symmetric model of wire arrays[2], which avoids the complications enumerated above by averaging over axial and azimuthal structure, and including other effects such as anomalous transport coefficients, within a fluid model. The report stresses the significance of anomalous resistive heating in accounting for the recent experimental results. In support of this point, a series of numerical experiments on the new WHYRAC code[3] are discussed. These extend our previous numerical studies[2], with the new code eliminating many shortcomings of the previous NRL wire code[4] (and other numerical treatments), e.g. the circuit is now treated exactly, separate electron and ion temperatures T_e and T_i are calculated, various forms of anomalous transport can be modeled, and radiative energy transport, including opacity effects, is treated more accurately than in any previous code of this type.

The outline of the report is as follows. In Section II we discuss relevant features of the recent experiments. In Section III, theoretical considerations are reviewed, and the significance of resistive heating is pointed out. In Section IV, we briefly introduce the WHYRAC code, and report on a recent series of studies with it. In Section V, we summarize and discuss the results.

II. Review of Experimental Results

Without going into details of machine characteristics, we describe here the aspects of the experimental results that are of particular interest with respect to the computer simulation. A typical time plot of the voltage in the pulse forming region in front of the Blumlein is shown in Fig. 1. This voltage pulse is dependent on the generator characteristics alone, and not on the specifics of the wire load. In Fig. 2, the current through the machine is plotted as a function of time. Classically the wire plasma is expected to form a low resistance and initially low inductance channel so that the current trace should be largely independent* of the specific wire array properties. This conclusion seems to be borne out in the experiments where the properties of the wire array do not markedly affect the current pulse. However, it should be recognized that the current measurement is usually taken at a position removed from the vicinity of the wire cage. What is measured is, in effect, a sum of the currents through the wire cage as well as possible currents across the electrodes in the vacuum feed region of the generator. Thus the apparent independence of the total current trace from the wire array properties does not prove definitively that the current through the wire plasma shares this property.

---

*The wire plasma inductance L_p increases as the wires implode, but typically does not dominate the circuit. However, the impedance due to dL_p/dt, is large enough to cause some modification of the current pulse at the time of assembly.

A time plot for radiated energy from an aluminum wire array, in the spectral region above 1 keV (Fig. 3), shows a rather simple structure. The density and temperature of an imploding plasma increases very rapidly just prior to the attainment of pressure equilibrium; an abrupt rise in the radiation flux is expected when this occurs. Subsequently, the radiating column is expected to expand and contract about its equilibrium position. The radiated power will fall during an expansion and rise during a contraction. This character is seen to occur in the decay part of the radiation pulse plotted in Fig. 3. The decay itself occurs when the coupling to the load decreases. The interesting feature of the radiation pulse from our point of view is that the value of the FWHM is 50-60 nsec. The effects of plasma column contractions and expansions of the radiated power are relatively minor. We feel that a major test of the validity of a numerical simulation is to yield the relatively broad radiation pulse found in the experiments.

The spectra observed in exploded wire experiments yield information on the average temperature and density of the wire plasma. Based on a particular opacity model, which is described in detail by Davis et al[5], it has been inferred from the spectra of several aluminum wire arrays that the x-rays with $h\nu > 1$ keV are emitted from a plasma region with average temperature and density about 550 eV and 3×10^{19} ions/cm^3, respectively. The opacity model was also used (in conjunction with a radiative transfer code) to calculate the radiated power from a uniform plasma with the inferred properties.

The calculated radiative output agreed with the experimental results when the diameter of the radiating column was taken to be 2mm, which is consistent with pinhole photographs estimates. This good agreement of both spectral properties and flux with observations confirms our confidence in the opacity model. The numerical simulations described below can thus be compared with the temperature and size of the radiation source region, as inferred by spectroscopic analysis of the experimental data.

III. Theoretical Considerations

The introduction of wire arrays instead of single wire in low-inductance machines was done originally to reduce the current rise time and to take advantage of the energy stored in the kinetic stage of implosion. A previous model[2] was developed for multiple wire dynamics, according to which the pinched plasma is heated by thermalization of the kinetic energy of implosion, and the radiation pulse occurs during a transient stage which terminates when this thermal energy is radiated away. Resistive heating was neglected during the radiation pulse, since it could be shown that classical resistance is negligible. However, recent experiments indicate the need for revisions in this model and strongly suggest that anomalous resistive heating occurs. In present high power machines, the anomalous resistive heating, instead of the kinetic energy of the implosion, seems to be the source of the radiated energy.

In this section, we shall recall the main features of our previous model and outline those new features that seem to be

indicated by recent experiments. It is assumed throughout this report that the wire plasma can be represented as azimuthally symmetric, i.e. that the existence of separate and distinct wires at early times can be ignored. For our purpose, then, the initial condition is one in which the plasma is cool and is located in a thin shell centered on the initial array radius. Previous computer simulations[6] indicated the following sequence of phenomena: (1) The plasma heats resistively to a few tens of eV (classical resistance is sufficient to do this). (2) The plasma properties (temperature, density profile) become essentially independent of the exact choice of initial conditions. The plasma shell thickness typically becomes larger than the final radius of the pinched plasma. (3) If the plasma resistivity is assumed to be classical, ohmic heating is found to be negligible at all later times, and the wire plasma resistance is negligible compared to other impedances in the generator/plasma circuit. (4) As the current increases, the magnetic pinch force increases and the plasma shell implodes. During this stage, energy input to the plasma is dominated by the Lorentz force, not by ohmic heating. In circuit terms, the rate of increase of plasma energy is

$$\dot{E} = \frac{1}{2} \dot{L}_p I^2 , \qquad (1)$$

where L_p is the plasma inductance. This energy input is to ion kinetic energy, but some of it is thermalized by shocks during the run-in. (5) When the plasma "assembles" - i.e. the hollow annulus

hits the axis, the plasma pressure is still too low to balance the magnetic pinch force. Pressure balance occurs[7] when

$$\langle (1 + Z)T \rangle = \langle 1 + Z \rangle T_B \equiv I^2/200k_B N_i, \qquad (2)$$

where T_B is the Bennett temperature in eV, N_i is the number of ions per cm length, I is the current in amps, and $k_B = 1.6 \times 10^{-12}$ ergs/eV is Boltzmann's constant. The imploding plasma overshoots pressure balance, and begins to "bounce" outward when

$$\langle T \rangle \approx 2\, T_B. \qquad (3)$$

At the bounce, the plasma kinetic energy is, by definition, at a minimum; nearly all the kinetic energy of the run-in has been thermalized. (6) The plasma radius r_p at the bounce (i.e. the minimum value of r_p), is determined by the requirement that the energy acquired during the run-in, from Eq. (1), equal the thermal energy $\frac{3}{2} N_i(1 + Z)\, T + \varepsilon_i N_i$, where ε_i is the mean energy invested in ionization and excitation (per ion). Use of Eq. (3) yields

$$\int dt\, \frac{1}{2} \dot{L}_p\, I^2 \approx 3\, N_i\, (1 + Z)\, T_B + 2\varepsilon_i N_i\,, \qquad (4)$$

and making the very simple estimate[2] $\varepsilon_i = \frac{1}{2} (1 + Z)\, T_B$, this relation reduces to

$$r_p \sim 0.15\, r_o\,, \qquad (5)$$

where r_o is the initial array radius. This gives $r_p \sim \frac{1}{2}$ mm to 2 mm for typical experimental parameters, and a mean ion density at peak compression $n_i \sim 3 \times 10^{20}$ cm^{-3} to 2×10^{19} cm^{-3}. (7) If radiative cooling is slow compared to the characteristic hydrodynamic time scale

r_p/c_s, where c_s is the sound speed (hydrodynamics-dominated regime), the plasma then oscillates about pressure balance, maintaining a temperature that varies from about 2 T_B to $\frac{1}{2}$ T_B. The plasma thermal energy $\sim 2\ N_i\ (1 + Z)\ T_B$, which derived originally from the kinetic energy of the run-in, is slowly radiated away. When this energy is used up, the plasma slowly collapses to higher density.[8] Radiation peaks correspond to times when the plasma is most compressed and hottest. (8) If radiative cooling is rapid (radiation-dominated or refrigerative regime), then the plasma cannot maintain $\langle T \rangle \gtrsim T_B$, and therefore fails to sustain pressure balance. In this case, the plasma collapses rapidly to very high density, cooling further by emitting copious, but mainly very soft, radiation.

For further elaboration of this model, the reader is referred to Ref. 2. The key point for our consideration here is that the hydro-dominated regime of this model showed qualitative agreement e.g. in plasma temperature and density, radiation fluence and radiation source radius, with the more successful Al multiple wire experiments on Owl II' and Blackjack III. But if a wire system evolved into a refrigerative collapse, the code predicted much less K-line radiation than was observed in the experiments.

The above model can only be successful when the radiation yields do not exceed the kinetic energy in the implosion. However, in the case of the new high power machines, it is clear that the radiated output greatly exceeds the implosion energy. Furthermore, voltage-current traces in the recent experiments (see Fig. 4) indicate that

the plasma impedance remains well-matched to the generator after plasma assembly, i.e. much of the energy is coupled into the plasma after assembly.

As discussed in Section II, the radiation pulse width is much longer than the hydrodynamic time scale characterized by the oscillations of the plasma column. This implies that the plasma radiates while it is in a quasi-steady-state, in which the plasma is maintained close to the Bennett temperature. If I is roughly constant during this stage, a steady state at roughly constant radius and density can be sustained only if a steady energy input balances the radiative cooling, keeping the plasma at T_B. This energy influx appears in the voltage-current traces as a resistive load, and within the limits of a one-fluid model can be interpreted as anomalous plasma resistance. Assuming that $\langle T_i \rangle = \langle T_e \rangle = T_B$, and further simplifying matters by assuming that the plasma temperature, density and current density are uniform, it is convenient to express the radiation flux as a factor $g_1(n, T_B)$ times the well-known Bremsstrahlung flux, and the resistivity η as a factor $g_2(n, T_B)$ times the classical (Spitzer) value; it can then be shown that the ratio of radiative energy loss rate $\dot{E}_{rad}$ to resistive heating rate $\dot{E}_{res}$ is

$$\frac{\dot{E}_{rad}}{\dot{E}_{res}} = \left(\frac{I}{I_{PB}(n, T_B)} \right)^2 ,$$

where I_{PB} is the Pease-Braginskii current,

$$I_{PB} = (1.6\ \text{MA}) \left(\frac{Z+1}{2Z}\right) \frac{g_2(n,T_B)}{g_1(n,T_B)} \left(\frac{\ell n\, \Lambda}{10}\right)^{\frac{1}{2}},$$

and $\ell n\, \Lambda \equiv 25.3 - 1.15\ \ln_{10} n_e + 2.3\ \ln_{10} T_e$ is the Coulomb logarithm. For our case, $(Z+1)/2Z \approx 0.5$ and $\ell n\, \Lambda \sim 8$.

We note that for classical resistivity and solely Bremstrahlung radiation,

$$I_{PB} \approx 0.71\ \text{MA}$$

becomes a constant, and a steady state can exist only at this current; if the current is higher, the plasma must collapse. What is more, radiation losses in addition to Bremsstrahlung further reduce I_{PB}. For higher currents, it is clear that <u>classical</u> resistive heating is negligible -- as assumed in our previous treatment -- and cannot support a steady-state. This suggests the existence of a large anomalous resistance, which can support such a steady state. For example, using our code results to determine g_1 in a typical case, we find that in order for I_{PB} to be equal to the measured current, the anomalous resistivity factor must be $g_2 \sim 20$. A higher value for g_1 (higher radiation level) will require a higher value for g_2 (anomalous resistivity) for a steady-state to be maintained.

In fact, these results point to the following trend for higher-Z materials. If a quasi-steady state is necessary to insure sustained radiation levels, and if the machines are operated at the same current level for various elements, the increase in anomalous resistivity will have to match the increase in radiated power as the atomic weight of the element increases. Mismatches may occur if the

anomalous resistivity does not increase, so as to match the particular radiative characteristics of a given high Z element, and in some cases a steady state, i.e. a sustained radiation pulse, may be attainable only by reducing the current. Unless anomalous resistivity is understood in physical terms, no scaling of the results presented here seems to be possible.

The assumption of anomalous resistivity also helps to explain the low density central pinch inferred experimentally. Such a soft pinch is possible if the pressure builds up in the center of the plasma annulus before assembly occurs. This can occur if the current penetrates the high-density plasma annulus, heating the annulus inner surface and causing it to expand toward the wire array axis. Continued current flow in this region heats it up significantly, and pressure balance is nearly achieved with the remainder of the plasma when it assembles. Current penetration to the central region will occur only if the characteristic magnetic diffusion time

$$\tau = \frac{4\pi\ell^2}{c^2\eta} \quad ,$$

where ℓ is the plasma annulus thickness, is no longer than the current rise time scale, i.e., a few tens of nsec. Based on Spitzer resistivity, current penetration in 20 nsec will occur, for ℓ = 1 mm, only if T $\lesssim$ 20 eV; but an anomalous resistivity factor g_2 = 50 allows current penetration to occur if T $\simeq$ 260 eV. Since this latter temperature is more typical of the temperature reached in the plasma during implosion, current penetration, central pressure build-up, and

consequent pinch softening is possible only if the resistivity is anomalously high.

In the next section, we shall discuss a series of numerical experiments, in which various forms of anomalous resistivity are introduced heuristically. We find that it is indeed possible in this way to generate code results that show qualitative agreement with the experiments. The possible sources of such anomalous resistivity are the subject of intense study, at present, and will be discussed in future reports.

IV. Numerical Studies

A. The WHYRAC Code

A one-dimensional code, WHYRAC[3], has been developed in order to study the dynamics of the multiple wire array. As discussed previously, the code provides a self-consistent treatment of the multiple wire plasma, based on the assumptions that: (a) The wire plasma can be adequately represented by an azimuthally symmetric model. This is well founded if the wire plasmas merge to form an annulus plasma early in the run-in stage[1], but could be qualitatively valid even if this does not occur. (b) Dependence on the axial variable z may also be ignored. (c) No current paths exist other than through the wire plasma.

WHYRAC is a one-fluid, two temperature code using FCT[9] to solve the fluid equations. It is Eulerian, but has variable mesh spacing and regridding capabilities that insure good resolution over the wide range of spatial scales that occur as the pinch ensues.

Circuit equations are solved self-consistently with the plasma variables, and the plasma is treated in an exact way as a circuit element. To handle radiative energetics (energy sources and sinks), an atomic physics/radiation transport package is called at each time step and solved self-consistently with the fluid and circuit equations. This package is a great advance over anything previously used in for this purpose in exploding wire studies, but the extent of detail included in it is limited by the requirement that it be rapid-running. In addition, a much more detailed and accurate atomic/radiation package[5] is used as a post-processor, to generate accurate spectra at less frequent intervals. Initially all the wire mass is taken to constitute a cool plasma distributed in an annulus near the original array radius - e.g. typically T = 1 eV, and annulus thickness 0.5 mm, although it is found that the results are insensitive to the exact choice of initial temperature and density profile. The essential input parameters are the wire material, wire mass, array radius, return current cage radius, transmission line impedance, vacuum feed inductance and either the voltage or current waveform. (The generator voltage wave form, taken from experimental data, is used as the input in the simulations reported here; a typical voltage trace is shown in Fig. 5). Output diagnostics provided by the code include radial profiles of n_i, n_e, T_e, T_i, radial velocity V, current density J, magnetic field B, axial electric field E, as well as radiation powers in lines and continuum in any frequency bin of

interest; for really accurate spectra, however, the post-processor is used.

B. Numerical Experiments

We shall discuss, for specificity, a series of numerical simulations that were carried out for a single set of typical experimental parameters with Aℓ plasma mass $1.14\ 10^{-4}$ g/cm, and the array radius r_o = 1.5 cm. In the different simulations, several of the transport coefficients were varied, as will be discussed.

In the first simulation, the resistivity was taken to be classical except that when the current flow speed $u \equiv |J/n_e e|$ exceeded the ion sound speed, the resistivity was increased to 100 times classical (Spitzer). This was intended to represent, in a very crude way, anomalous resistance due to the well known streaming instabilities - particularly the modified two-stream and (if $\sim T_e >> T_i$) ion sound. It has been shown in a series of papers[10] that in this type of situation, it is not the exact value of the anomalous transport coefficient that is crucial but only the fact that the instability turns on at a certain value of u and that resistivity becomes very large for larger values of u; the system typically adjusts itself so that u always remains at the critical - i.e. marginally stable - value.

Time dependence of the total thermal, kinetic, and radiated energies, as well as of the maximum density at a given time, are shown in Fig. 6. We note that the behavior is that of the "refrigerative" mode, where the plasma collapses abruptly to very high

density, because of radiative losses. The temperature falls well below T_B as this happens. As shown in Fig. 7, line radiation, particularly the K-line radiation at $h\nu \sim 1.7$ keV, falls rapidly after an initial peak; thus the K-line radiation pulse of interest is very short ($\sim$5 nsec). Continuum radiation, whose rate scales as density, since the plasma is optically thin to it, dominates the energy loss in the dense cool state. The main effect of anomalous resistance, of the type introduced here, is simply to prevent current flow speeds $u >> c_s$, and thereby to prevent the current from flowing heavily in low density regions on the outside of the plasma. Since the current then flows predominantly in dense plasma where $u < c_s$, anomalous resistive heating is unimportant, and fails to prevent the refrigerative collapse.

Density and temperature profiles at t = 110 nsec (when the radiation spike ends) are shown in Fig. 8. The central region is at high density ($n_i \sim 10^{21}$ cm^{-3}) and is already quite cold. Radiation originates predominantly in this region, and is dominated by continuum. A surrounding region of plasma is at very low density ($n_i \sim 5 \times 10^{17}$ cm^{-3}) and T $\sim$ 4.5 keV, while the very low density outer corona attains still higher temperatures. This compares poorly with the experimental results, which show: (1) a radiation pulse duration $\sim$tens of nanoseconds, (2) a radiating region of moderate density $n_i \sim 3 \times 10^{19}$ cm^3 and fairly high temperature, $T_e \sim 500$ eV, as inferred by spectroscopy; (3) harder radiation emanating mainly from a central region and softer radiation from the outer region; (4) much more K-line radiation than

is predicted by the code; (5) little or no dip in the current trace at the time of assembly, as compared to a strong dip in the computer simulation (due to a very large rate of change of plasma inductance $\dot{L}_p$ during the plasma implosion).

From the discussion of Sec. III, it seems likely that the poor agreement of the computer simulation with experiment is due to the inadequacy of resistive heating to support a steady state. The central core plasma, in particular, fails to heat sufficiently to achieve pressure balance. We have proceeded on the hypothesis that the fundamental framework of the calculational model (fluid, with only radial dependence) is reasonable, but that other effects which are not presently well understood can result in changes in the effective transport coefficients. Thus we modify these coefficients in a sequence of well defined ways to study their effect on the results: (1) In order to enhance penetration of heat into the core, and thus possibly soften the assembly, thermal conductivity was increased by up to a factor of 80 over the classical value. No significant change in the results occurred. (2) For $u > c_s$, the anomalous resistance was increased to 1000 times the classical value. No significant change occurred, thus supporting the marginal stability picture that the numerical value of the anomalous transport coefficients values does not play a crucial role, once the instability threshold is computed accurately. (3) Although we believe that radiative emission is well modeled in WHYRAC, we tested the sensitivity of the results to the line radiation rate (due to the uncertainty in opacity values) by

decreasing this rate by a factor up to 40 for all the lines. No essential change in the refrigerative collapse occurred. Continuum radiation was sufficient to cause the collapse. (4) A large anomalous resistivity was imposed everywhere, even when the current drift speed u was small. For simplicity, this anomalous resistivity was assumed to be of the form of a constant g_2 times the classical resistivity $\eta(T)$. For a wide range of choices of g_2, this assumption completely changes the results, leading to evolution that shows qualitative agreement with the experimental results, i.e. the plasma persists in quasi-steady equilibrium after assembly, with $\langle T \rangle$ oscillating gently about T_B, and with much of the radiation emitted in lines at $h\nu > 1$ keV. The time evolution of one such simulation, with the choice $g_2 = 50$, is shown in Fig. 9. In Fig. 10, we note that the radiation pulse has been broadened significantly. Furthermore, the temperature and density profiles of Fig. 11, at t = 113 nsec (near the time of peak radiation rate), show a plasma radius ~1.5 mm, in reasonable agreement with Eq. (5) and with the experiments, and a detailed structure with a hot central core ($n_i \sim 5 \times 10^{18}$ cm^{-3}, $T_e \sim 3$ keV, radius ~ 1mm) surrounded by a warm, somewhat denser outer ring ($n_i \sim 3 \times 10^{19}$ cm^{-3}, $T_e \sim 500$ eV). This type of structure agrees with the experimental observations that the harder radiation is emitted from the core. Also, the K-line radiation in the simulation is emitted principally from the outer region, whose temperature and

density agree reasonably well* with the values inferred spectroscopically from the experimental data. The dip in the current trace I(t) at assembly, in Fig. 13, is seen to be much weaker than the corresponding dip for $g_2 = 1$ (in Fig. 12), since the rapid refrigerative collapse does not occur. Thus, this simulation shows good general agreement with experiment.

The results described above do not change drastically for choices of g_2 up to 80; on the other hand $g_2 = 10$ results in a refrigerative collapse similar to that for $g_2 = 1$. The reason for this would appear to be that the radiation rate at $\langle T \rangle = T_B$ exceeds the classical resistive heating rate by a large factor of order 20. If the resistive heating rate is enhanced by exactly this factor, a genuine steady state occurs; but if the resistive heating rate is merely close to the radiative cooling rate, a quasi-steady state with $\langle T \rangle = T_B$ occurs, in which the plasma slowly expands (or contracts) in such a way that the adiabatic cooling (or heating) is just sufficient to maintain $\langle T \rangle = T_B$. On the other hand, if the radiative cooling rate far exceeds the resistive heating rate, the collapse is sudden and refrigerative, rather than quasi-steady.

As a further test on the significance of anomalous resistance, some additional computer simulations were run, in which the anomalous resistivity factor $g_2 = 50$ was turned on at a time $t_1 \neq 0$. We found

---

*Some spectral details indicate that the experimental plasma is moderately hotter than the temperature seen in the simulations.

that for $t_1 \lesssim 70$ nsec the results were the same as for $t_1 = 0$, i.e. the anomalous resistance simulations just described. On the other hand, anomalous resistance turned on at $t_1 > 90$ nsec failed to prevent the refrigerative collapse (although it is likely that the plasma would eventually have heated up again and come to pressure balance, if it were run long enough). We conclude that the effects of anomalous resistance at early times (e.g. increased current diffusion and heating of the interior plasma) are unimportant to the phenomena under discussion, but the effects of anomalous resistance during the implosion and afterwards are all-important.

V. Conclusions

It has been shown that one-dimensional (radial) fluid models with classical transport coefficients agree poorly with the results of recent high-power multiple wire experiments. The introduction of anomalous resistance only when the current flow velocity u is high, based on the marginal stability picture of current-driven instabilities, fails to correct the inadequacies of the model. However qualitative agreement with the experiments is found when a large anomalous resistivity is introduced, which persists at low current flow velocity. This situation is similar to that in post-implosion theta pinches, where it is believed that lower hybrid instabilities are responsible for anomalous resistance at low u,[11] and in plasma focuses, where anomalous resistance also appears to occur[12], for reasons which are not understood. Wire arrays on the present generation of low-inductance machines do not operate as they were

initially thought to (conversion of kinetic energy of implosion into radiative energy). In order to calculate the essential plasma heating process, and generate useful scaling laws, we believe that the anomalous resistance must be understood in detail. In particular, a sustained radiation pulse seems to require a balance between radiation flux and resistive heating; thus, prediction of optimum currents for various wire materials requires an understanding of how both of these quantities scale with Z and (through the condition $T = T_B$) with I.

The introduction of anomalous resistance into the transport simulates qualitatively the performance of the present machines within the limits of a one fluid model, in that

a) it provides an energy flow into the plasma after assembly, driving the radiation pulse, and

b) a high pressure forms at an early time on the axis of the wire array, preventing a total collapse of the wire plasma and softening the pinch.

Since the results of this paper point to the importance of anomalous transport, the detailed theory of various non-fluid transport mechanisms will be studied in future work. We conclude this paper with a few comments along these lines. In addition to the micro-instabilities which are traditionally regarded as the source of anomalous resistance, such as lower hybrid instability[10] (which continues to operate at low current flow speed), a number of non-fluid phenomena are probably occurring in high-power wire plasmas, which may eventually be modeled as anomalous transport coefficients

or energy sources and sinks within the framework of a code like WHYRAC. The deposition of energy in the wire plasma by field emitted electrons or high-energy ions could be included in this way (although a separate diode code would be needed to calculate the evolution of such high-energy particles). Runaway electrons are likely to occur in the plasma, since the Dreicer critical field

$$E_{cr} = 2.69\,\Lambda\, Z\, e^3\, n_e/T_e$$

is only $E_{cr} \approx 1.2 \times 10^5$ V/cm in the hot, low-density core shown in Fig. 11; the axial electric field easily exceeds E_{cr} in this case. The generation of suprathermal electrons would have to be treated self-consistently with the instabilities responsible for anomalous resistance. The ion Larmor radius approaches (and the mean free path exceeds) the characteristic dimensions of the pinched plasma in some high temperature regions; correct treatment may require the use of a hybrid kinetic-ion/fluid-electron picture, as has proven necessary in recent theta pinch work.[13] These and several other approaches to non-classical-resistive heating are presently being studied, because of the strong indication from these studies that they play a crucial role.

References

1. M. Lampe, H. Bloomberg, D. Colombant, "Behavior of an Exploding Wire at Early Times", NRL Memorandum Report (to be published).
2. M. Lampe, J. Davis, D. Mosher, D. L. Book, R. Lee and H. Bloomberg, unpublished.
3. D. G. Colombant, M. Lampe and H. W. Bloomberg, "WHYRAC- A New Modular One-Dimensional Exploding Wire Code", NRL Memorandum Report 3726 (1978).
4. D. Mosher, S. J. Stephanakis, K. Hain, C. M. Dozier and F. C. Young, Annals New York Academy of Science 251, 632 (1975).
5. J. David, P. C. Kepple and J. P. Apruzese, to be published.
6. See Ref. 2; also Sec. IV of the present report.
7. L. Spitzer, Jr., "Physics of Fully Ionized Gases", Interscience Publishers p. 109 (1962).
8. J. Shearer, Phys. Fluids 19, 1426 (1976).
9. J. P. Boris and D. L. Book, J. Comp. Phys. 11, 38 (1973).
10. M. Lampe, W. M. Manheimer and K. Papadopoulos, "Anomalous Transport Coefficients for HANE", NRL Memo. Report 3076 (1975); W. M. Manheimer and J. P. Boris, Comments Plasma Phys. Cont. Fusion 3, 15 (1977).
11. R. C. Davidson and N. T. Gladd, Phys. Fluids 18, 1327 (1975). R. C. Davidson, N. T. Gladd, C. S. Wu and J. D. Huba, Phys. Rev. Lett. 37, 750 (1976); P. C. Liewer and R. C. Davidson, Nuc. Fusion 17, 85 (1977).

12. J. de Mascureau, A. Bernard, J. P. Garconnet and A. Jolas, Bull. Am. Phys. Soc. 22, 1063 (1977).

13. P. C. Liewer, Nucl. Fusion 16, 817 (1976).

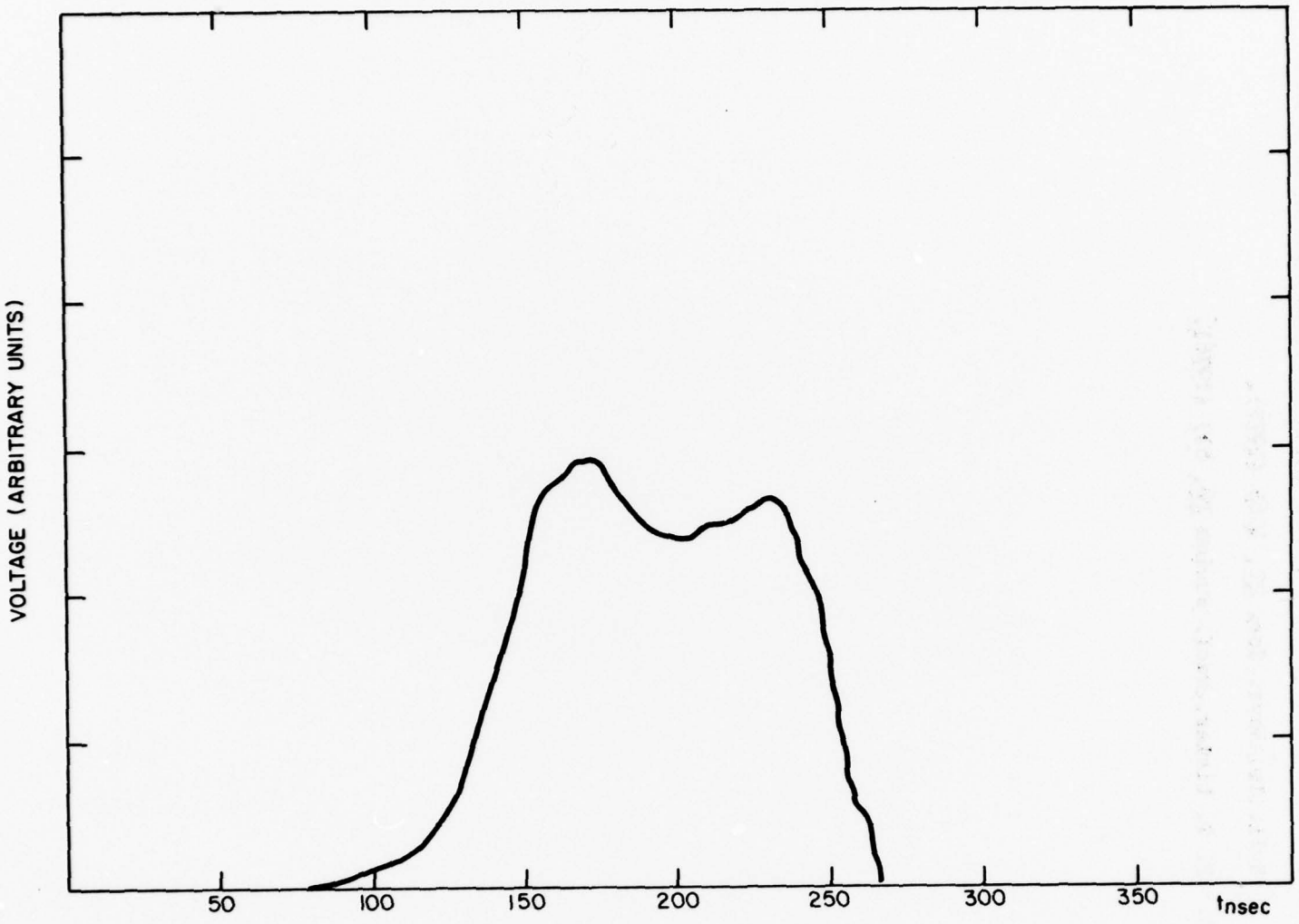

Figure 1. Typical tube voltage (in arbitrary units) as a function of time.

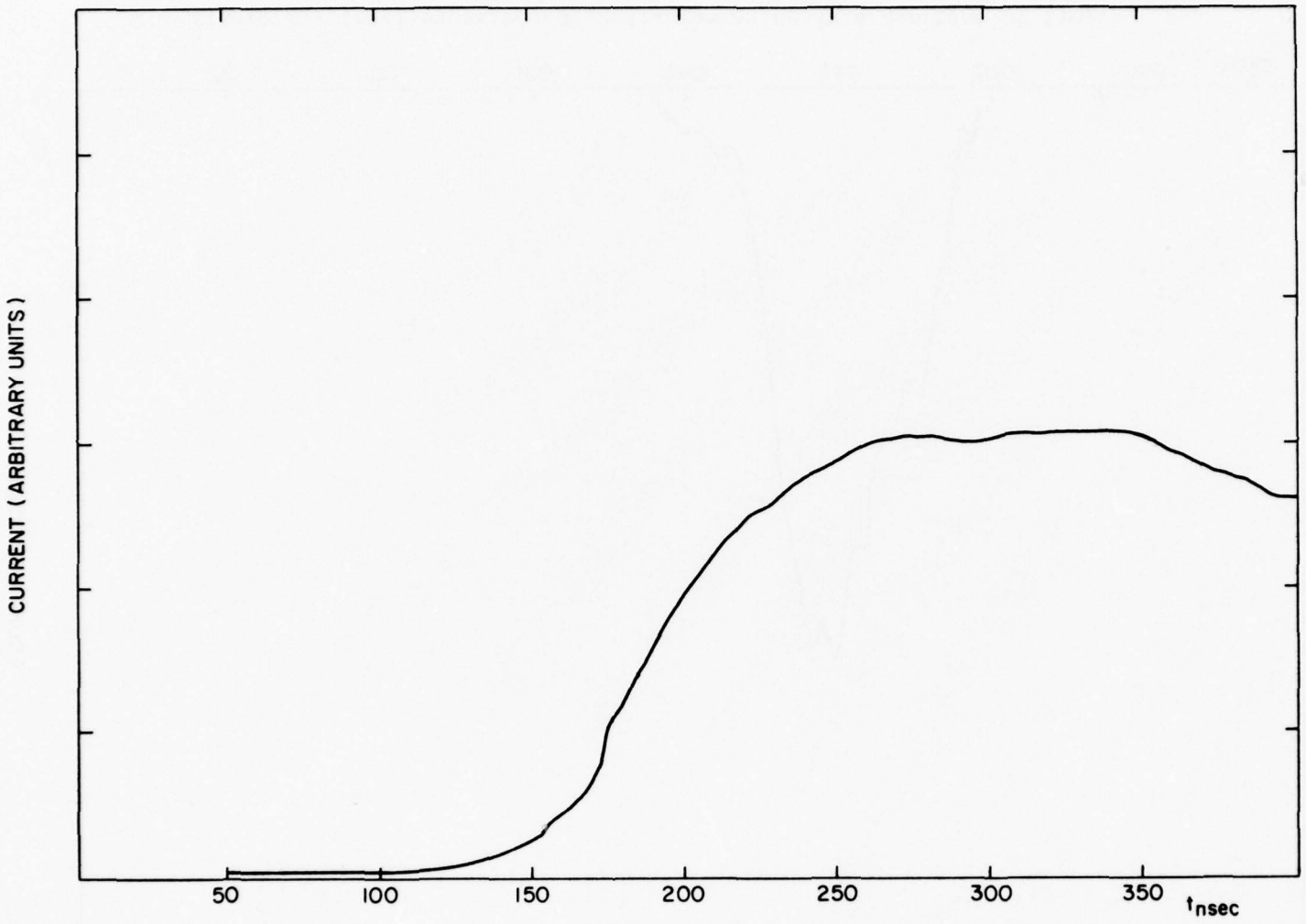

Figure 2. Typical experimental current trace (in arbitrary units) as a function of time.

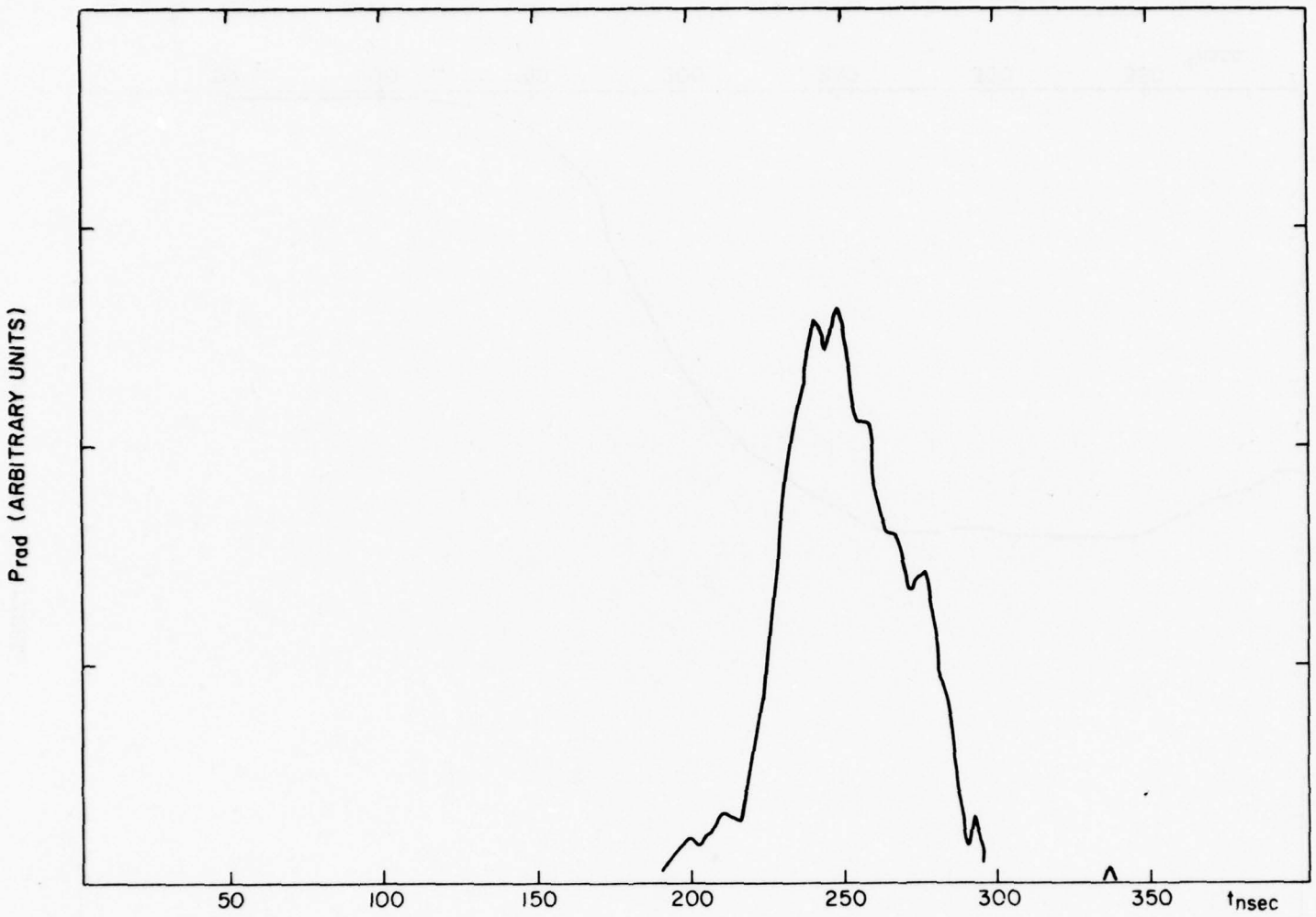

Figure 3. Total experimental radiation pulse as a function of time.

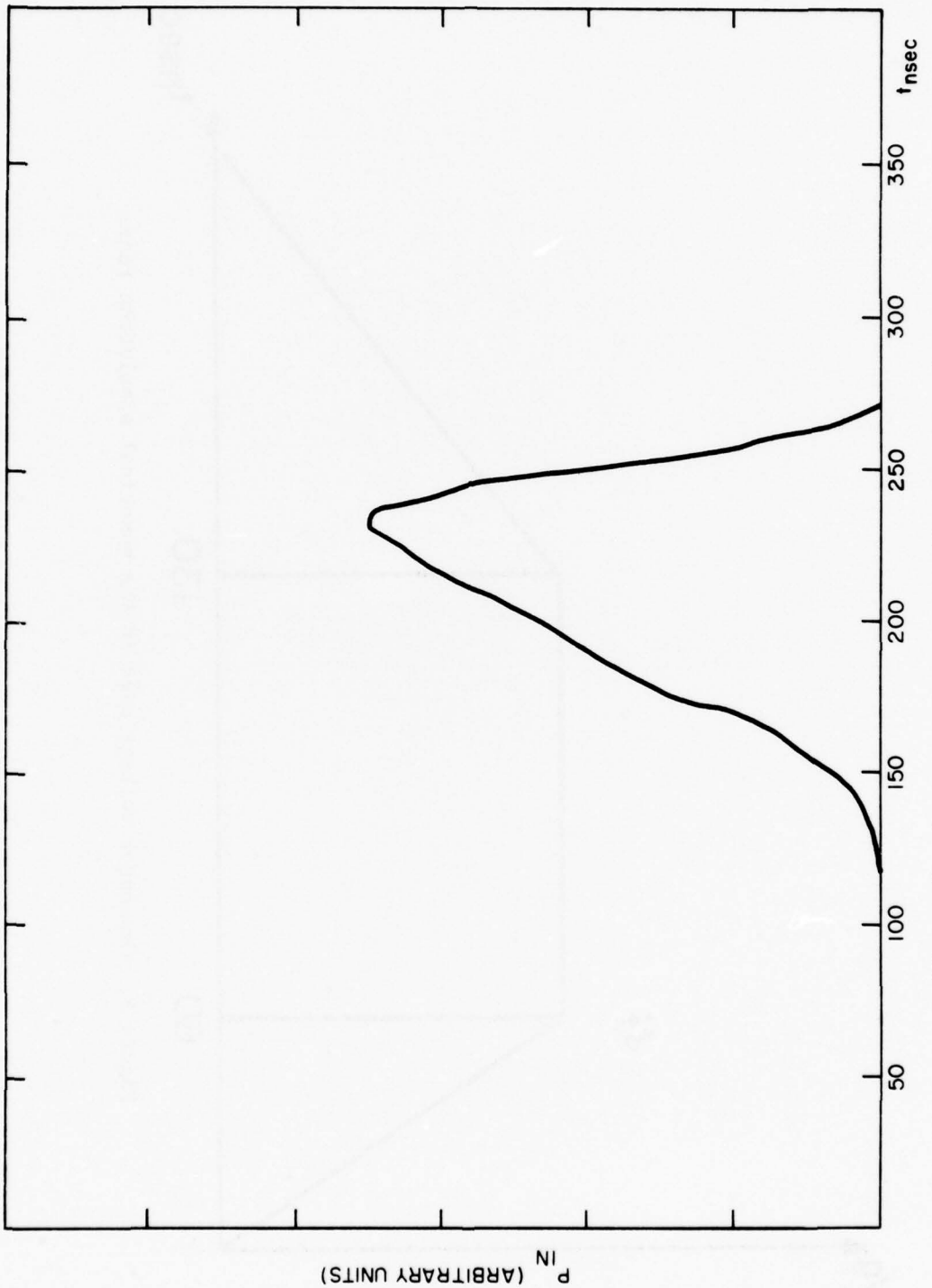

Figure 4. Input power corresponding to same shot.

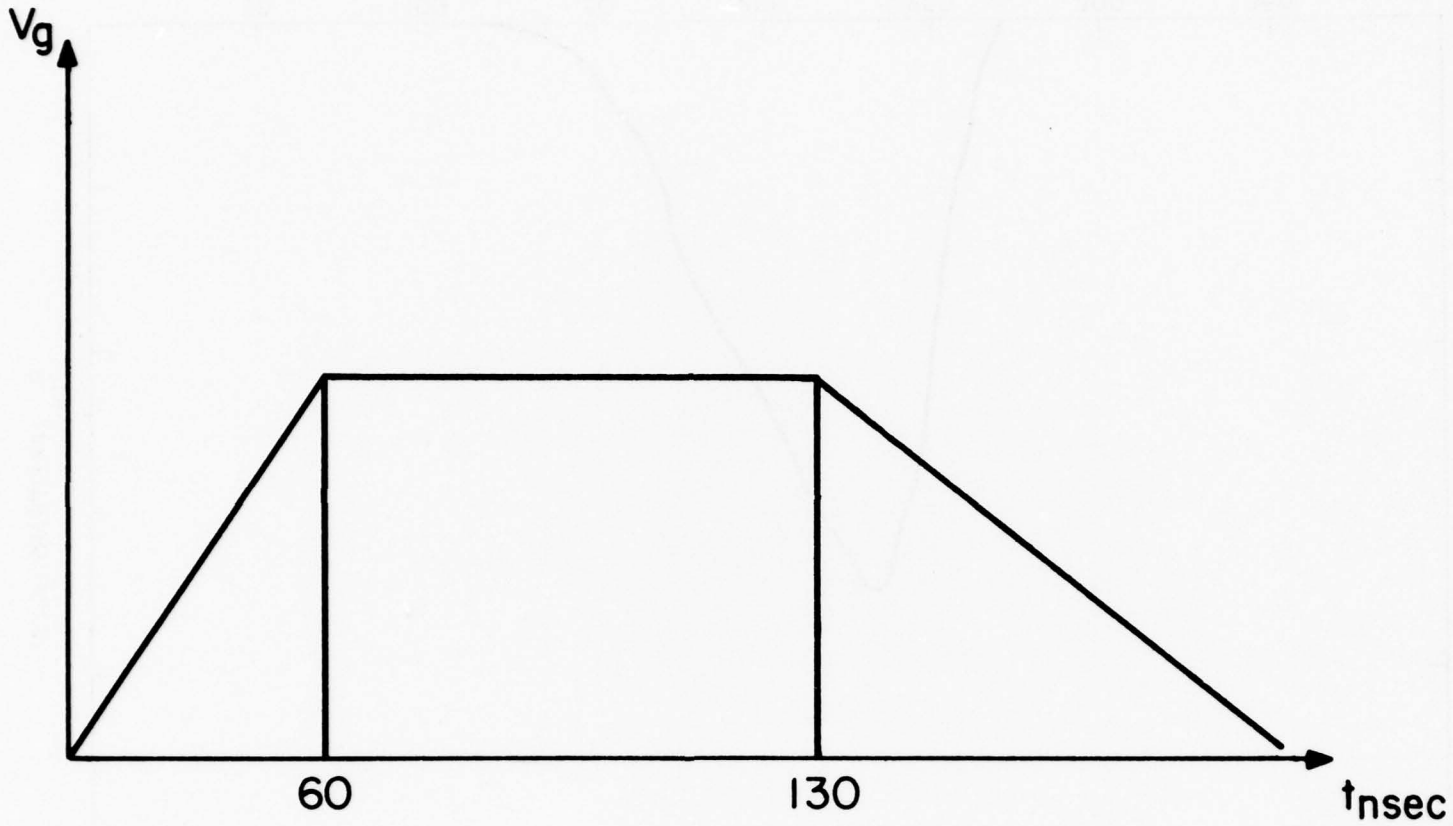

Figure 5. Generator voltage used in the numerical simulation runs.

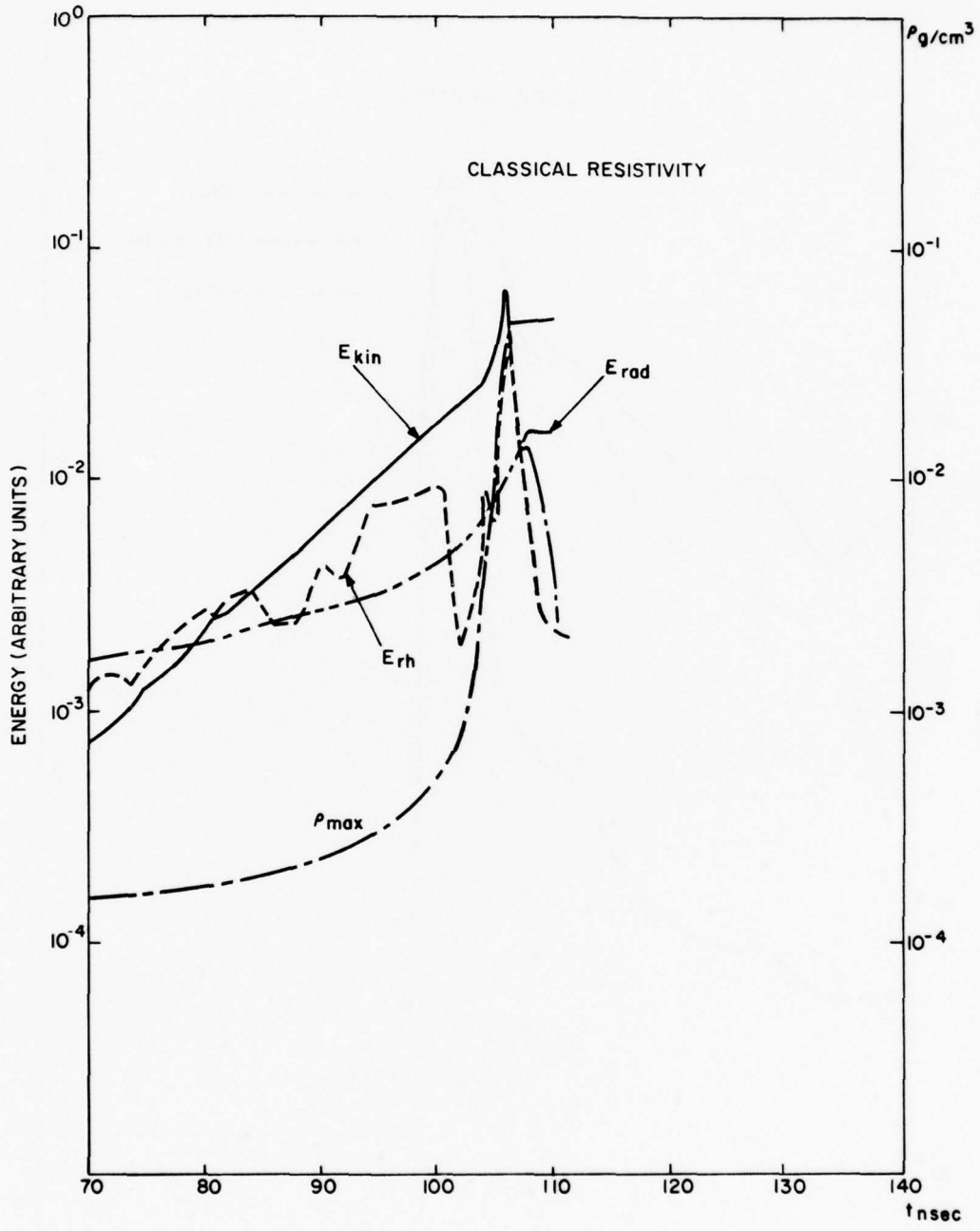

Figure 6. Kinetic, thermal and radiated energies as a function of time for classical resistivity run. Also, maximum density curve, showing strong pinching occurring at assembly.

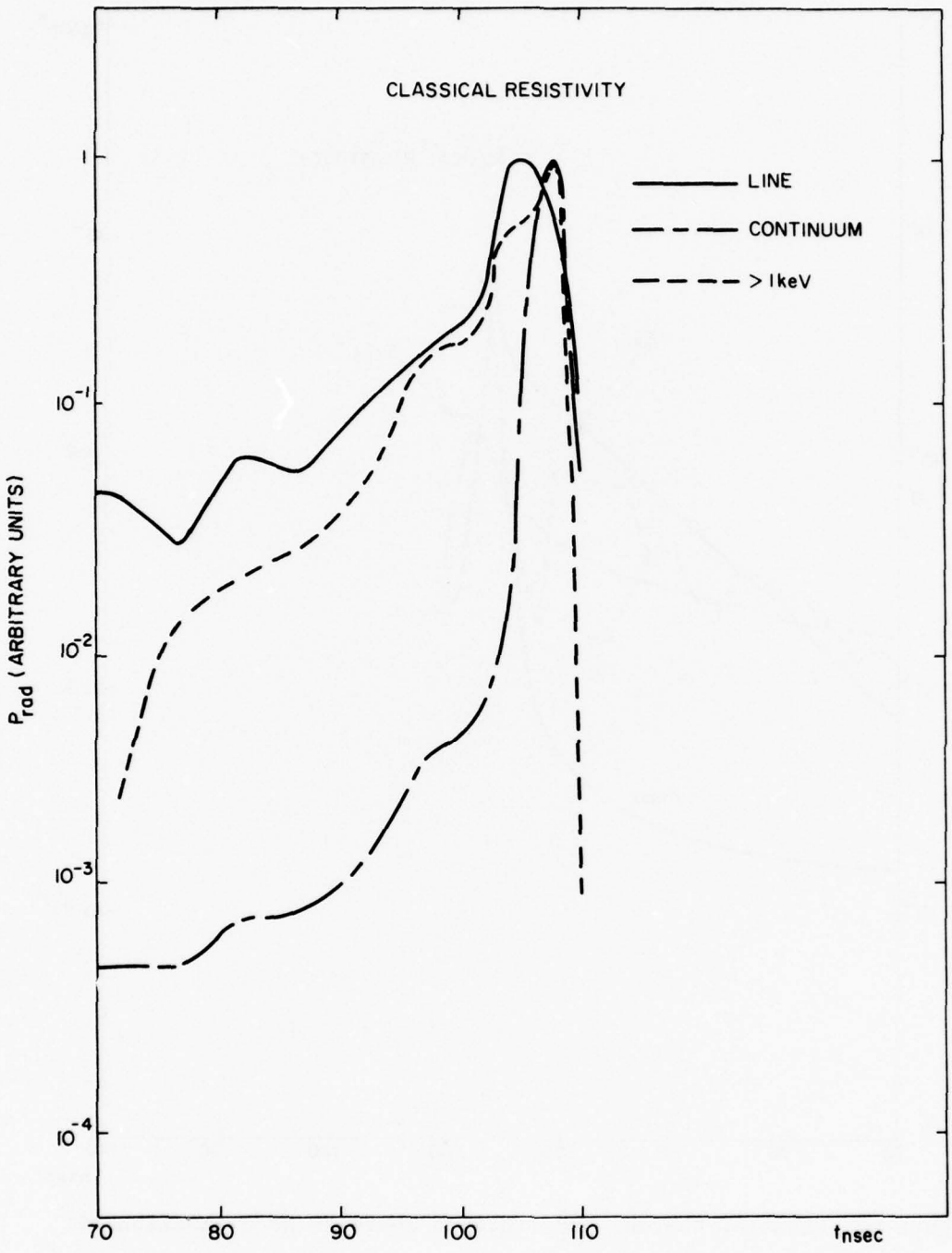

Figure 7. Radiated powers as a function of time for classical resistivity run. (Arbitrary units -- each curve is normalized to its own maximum value.)

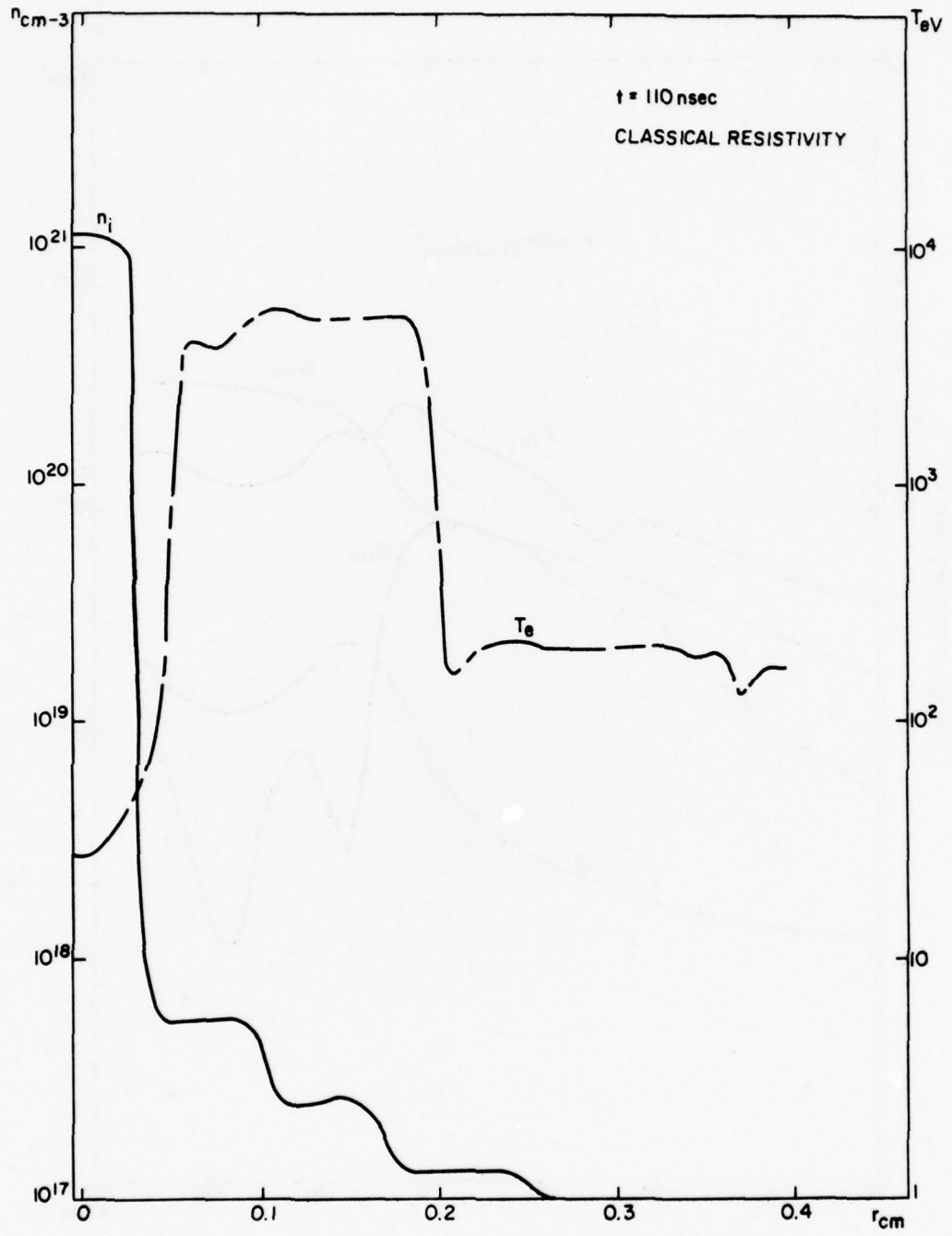

Figure 8. Electron temperature and ion density profiles as a function of radius at time near assembly for classical resistivity run. Note high axial ion density and low axial electron temperature.

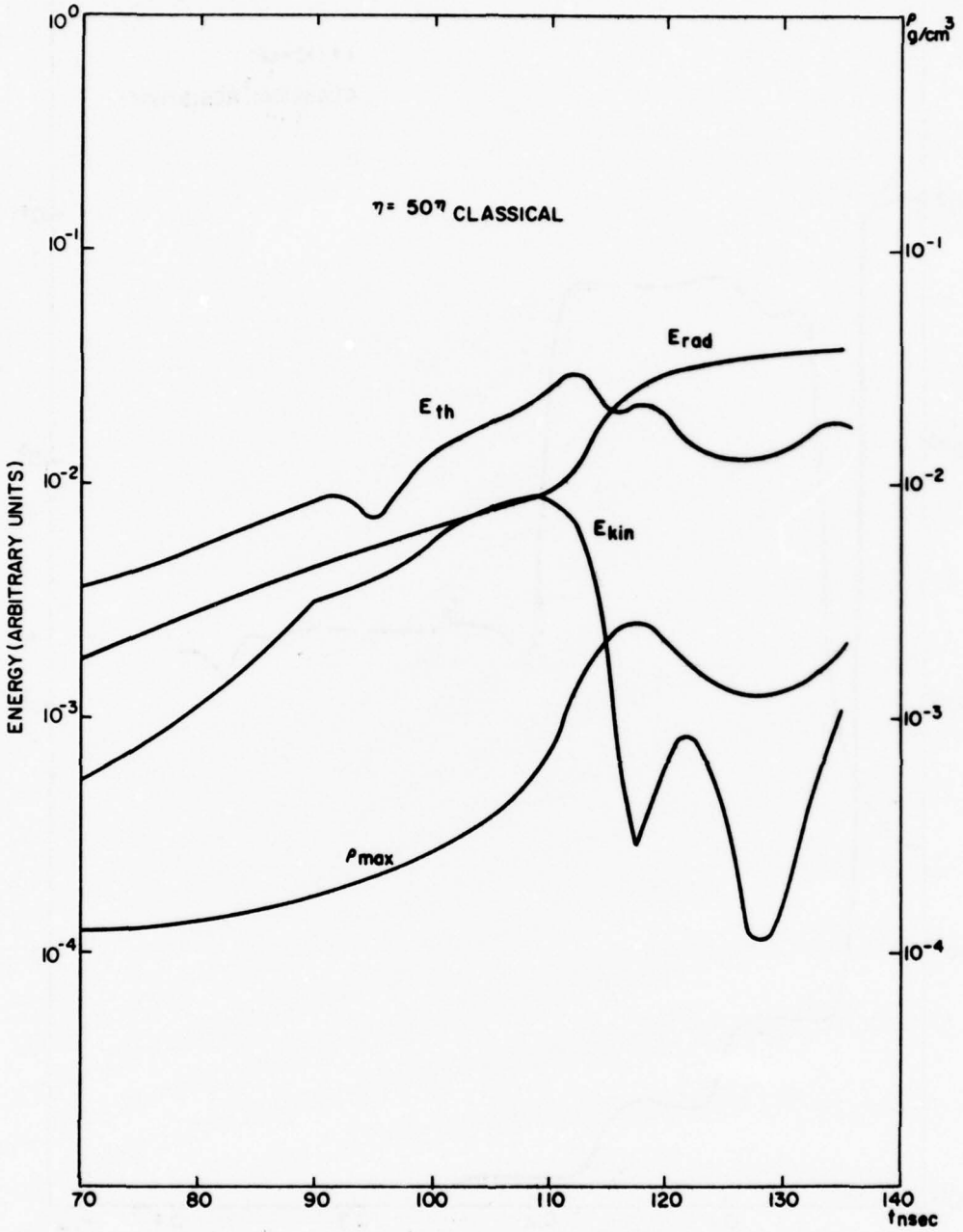

Figure 9. Same plot as Fig. 6 but for an anomalously enhanced resistivity everywhere in the plasma. (50 times classical resistivity).

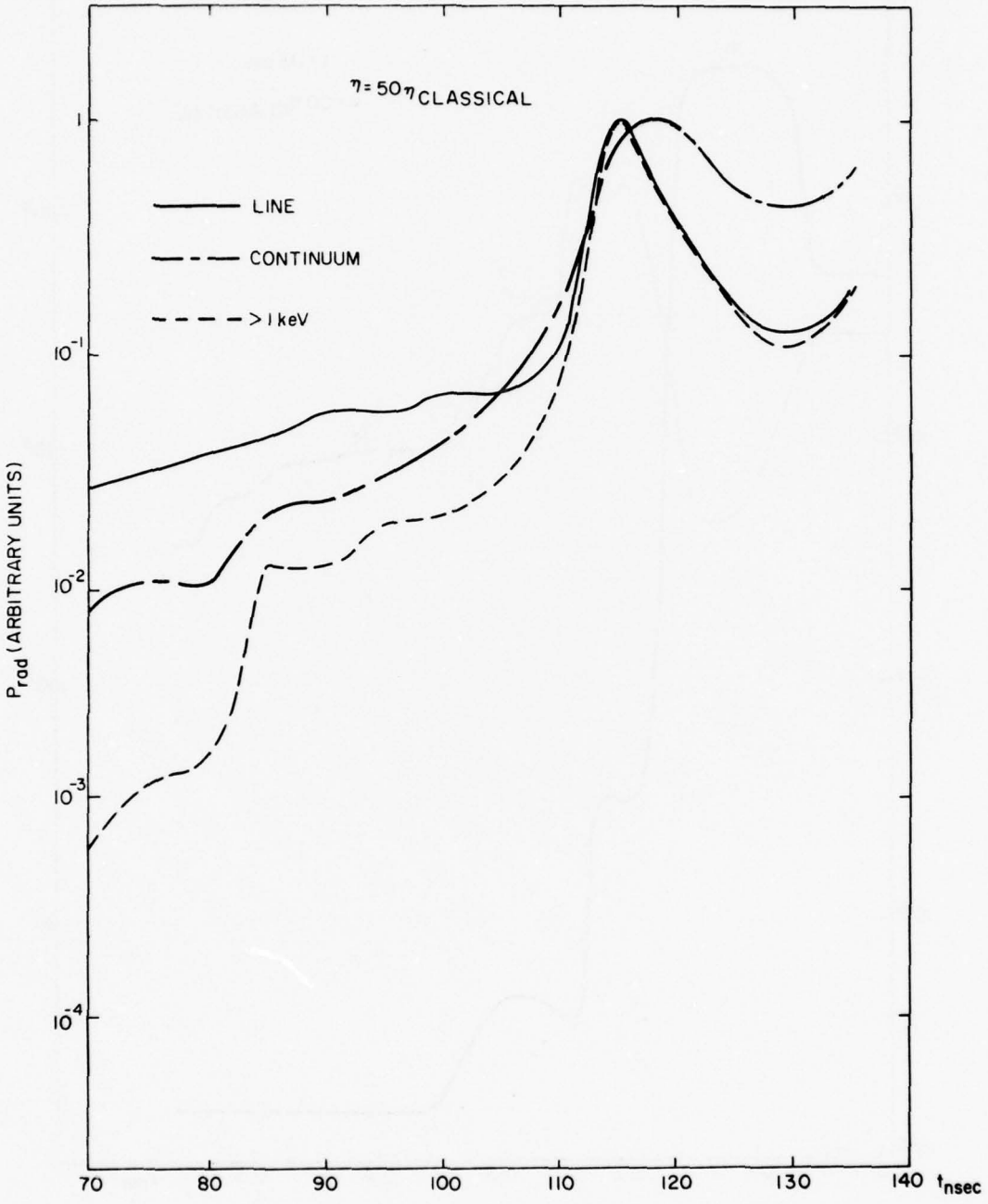

Figure 10. Radiated powers as a function of time for anomalous resistivity run. (Arbitrary units--each curve is normalized to its own maximum value.)

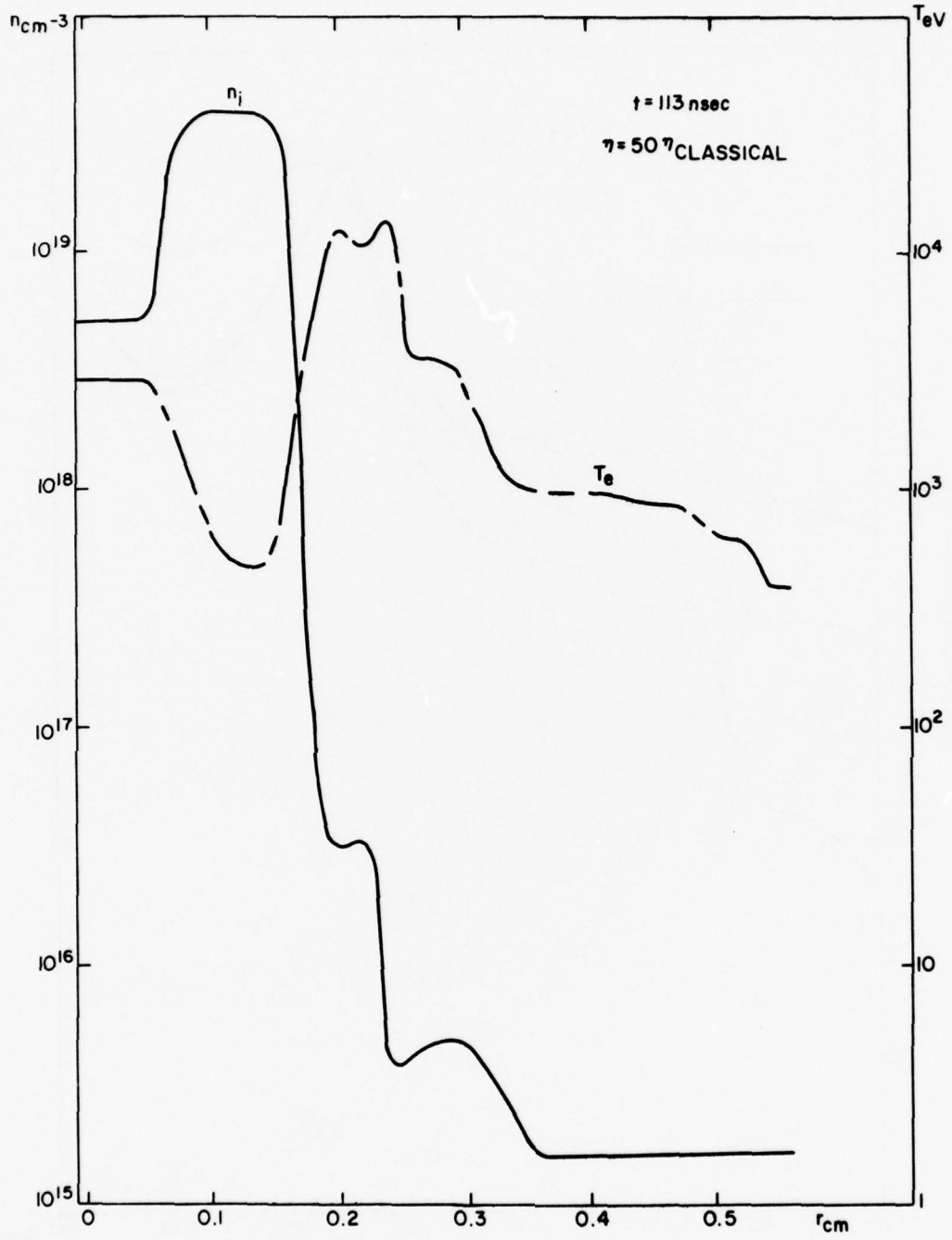

Figure 11. Electron temperature and ion density profile as a function of radius near assembly for anomalous resistivity run. Note structure and magnitude of ion density near axis as well as electron temperature.

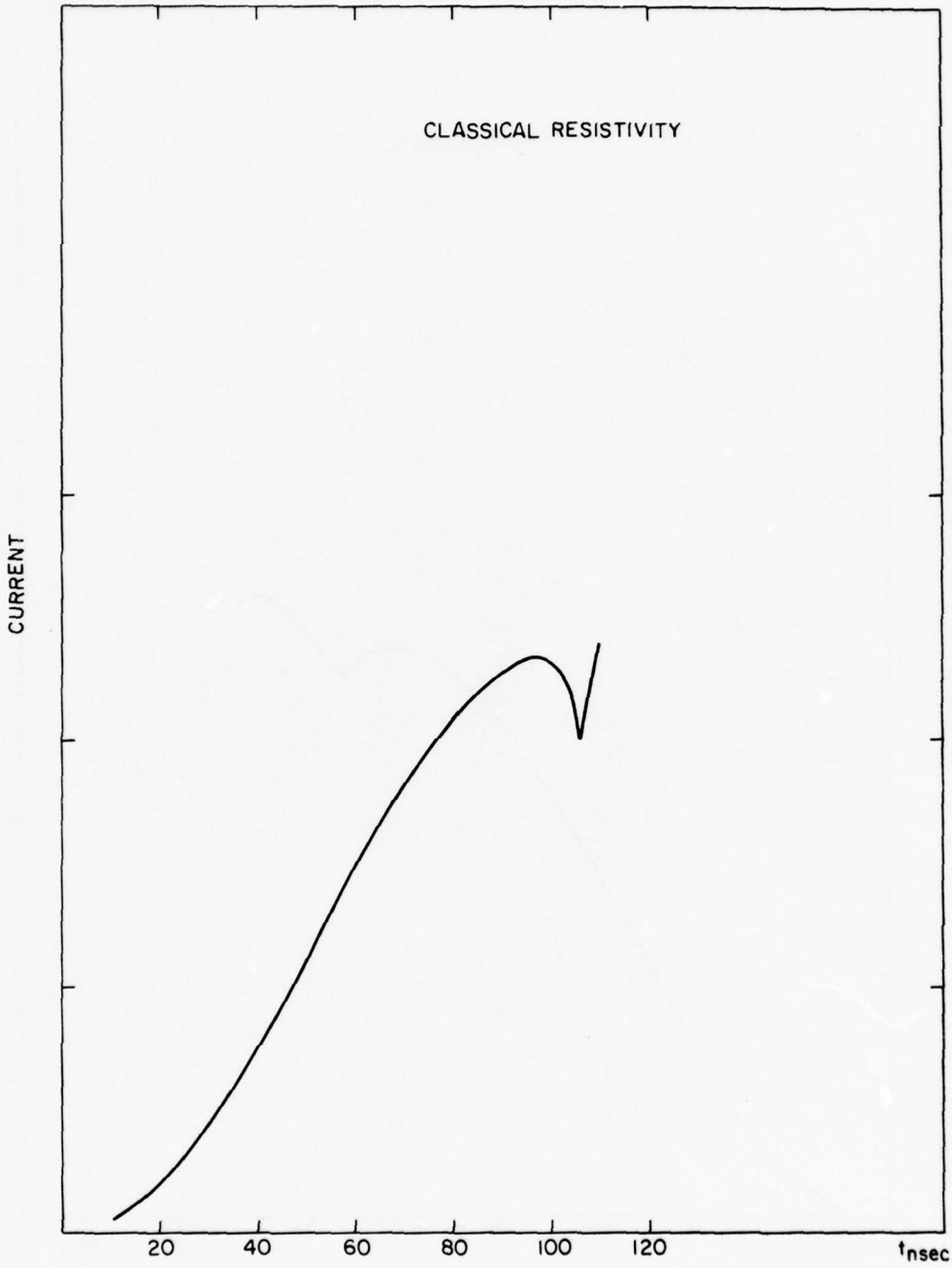

Figure 12. Current trace for classical resistivity run as a function of time. Dip indicates pinching. (Arbitrary units).

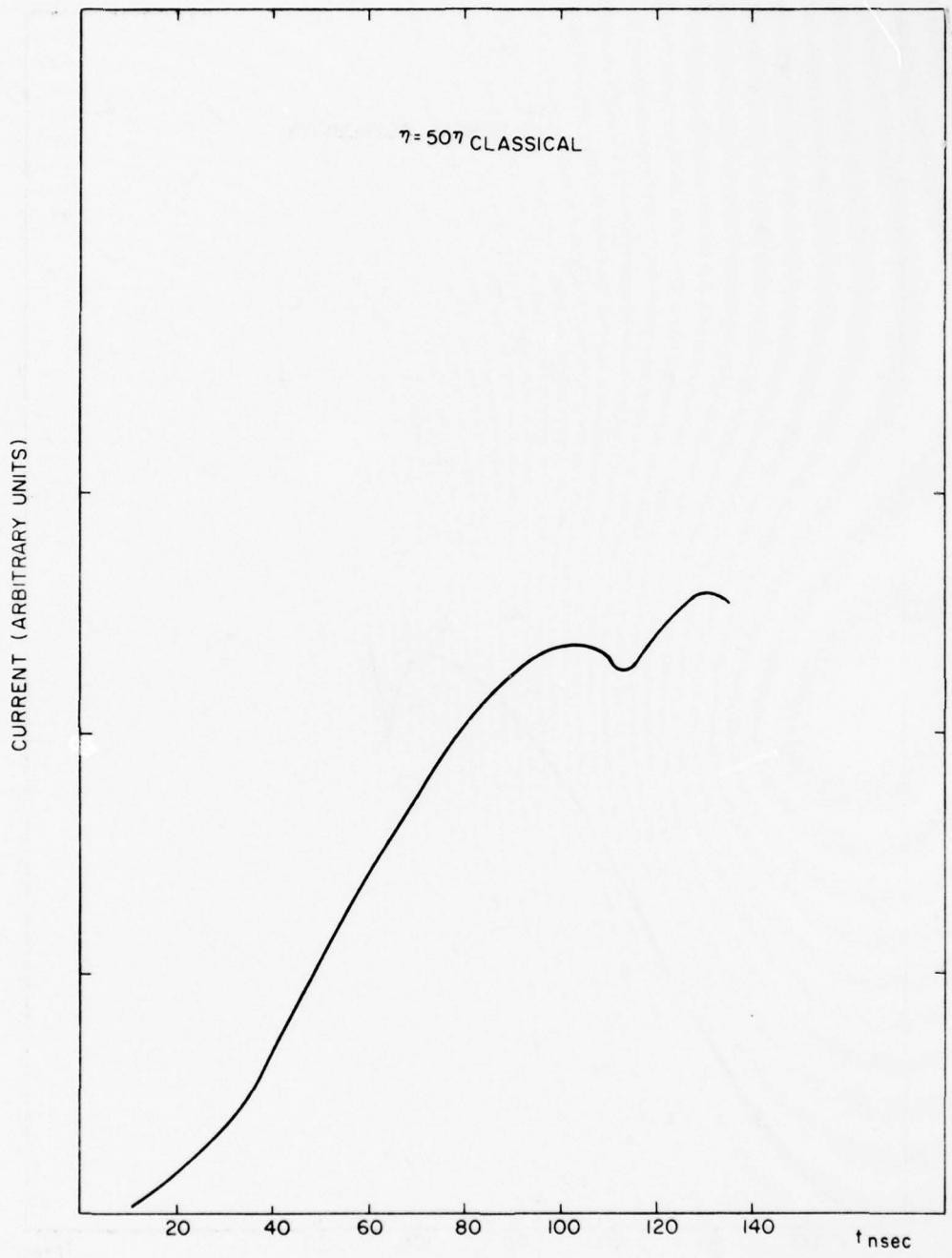

Figure 13. Current trace for anomalous resistivity run as a function of time. (Arbitrary units). Dip in current is smoother than for classical resistivity run.

DISTRIBUTION LIST

DIRECTOR
Defense Advanced Rsch Proj Agency
Architect Building
1400 Wilson Blvd.
Arlington, Va. 22209
ATTN: Strategic Tech Office

Defense Communication Engineer Center
1860 Wiehle Avenue
Reston, Va. 22090
ATTN: CODE R820 R. L. Crawford
ATTN: Code R410 W. D. Dehart

DIRECTOR
Defense Communications Agency
Washington, D. C. 20305
ATTN: CODE 960
ATTN: CODE 480

Defense Documentation Center
Cameron Station
Alexandria, Va. 22314 — 12 copies (if open publication)
ATTN: TC — 2 copies (if otherwise)

DIRECTOR
Defense Intelligence Agency
Washington, D. C. 20301
ATTN: W. Wittig DC - 7D
ATTN: DT-1B

DIRECTOR
Defense Nuclear Agency
Washington, D. C. 20305
ATTN: STSI Archives
ATTN: STVL
ATTN: STTL Tech Library — 2 copies
ATTN: DDST
ATTN: RAAE

DIR OF DEFENSE RSCH & ENGINEERING
Washington, D. C. 20301
ATTN: DD/S&SS John B. Walsh
ATTN: OAD/EPS

COMMANDER
Field Command
Defense Nuclear Agency
Kirtland AFB, NM 87115
ATTN: FCPR
ATTN FCPR COL. John P. Hill
Interservice Nuclear Weapons School
Kirtland AFB, NM 87115
ATTN: Document Control

DIRECTOR
Joint Strat TGT Planning Staff Jcs
Offutt AFB
Omaha, NB 68113
ATTN: JLTW-2
ATTN: JPST G. D. Burton
ATTN: JPST MAJ. J. S. Green

CHIEF
Livermore Division Fld Command DNA
Lawrence Livermore Laboratory
P. O. Box 808
Livermore, CA 94550
ATTN: FCPRL

COMMANDER
National Military Comd Sys Support Ctr
Pentagon
Washington, D. C. 20301
ATTN: B211
ATTN: DP DIRECTOR FOR CSPO

DIRECTOR
National Security Agency
Ft. George G. Meade, Md. 20755
ATTN: W14 Pat Clark
ATTN: Frank Leonard

OJCS/J-3
The Pentagon
Washington, D. C. 20301
ATTN: J-3 OPS ANAL BR. COL. Longsberry

OJCS/J-6
The Pentagon
Washington, D. C. 20301
ATTN: J-6

DIRECTOR
Telecommunications & Comd & Con Sys
Washington, D. C. 20301
ATTN: ASST DIR Info & Space Sys
ATTN: DEP ASST. SEC Sys

Weapons Systems Evaluation Group
400 Army-Navy Drive
Arlington, Va. 22202
ATTN: DOCUMENT CONTROL

COMMANDER
Harry Diamond Laboratories
2800 Powder Mill Road
Adelphi, Md. 20783
ATTN: AMXDO-NP

COMMANDER
TRASANA
White Sands Missile Range, NM 88002
ATTN: EAB

DIRECTOR
U. S. Army Ballistic Research Labs
Aberdeen Proving Ground, Md. 21003
ATTN: AM-CA Franklin E. Niles

U. S. Army Communications CMD
C-B Services Division
Pentagon Rm. 2D513
Washington, D. C. 20310
ATTN: CEAD

COMMANDER
U. S. Army Electronics Command
Fort Monmouth, N. J. 07703
ATTN: AMSEL-TL-ENV Hans A. Bomke

COMMANDER
U. S. Army Material Command
5001 Eisenhower Avenue
Alexandria, Va. 22333
ATTN: AMCRD-WN-RE John F. Corrigan

COMMANDER
U. S. Army Material Command
Foreign and Scientific Tech Center
220 7th St. N. E.
Charlottesville, Va. 22901
ATTN: P. A. Crowley
ATTN: R. Jones

COMMANDER
U. S. Army Missile Command
Redstone Arsenal
Huntsville, Al. 35809
ATTN: AMSMI-YTT W. G. Preussel, Jr.

COMMANDER
U. S. Army Nuclear Agency
Fort Bliss, Tx. 79916
ATTN: USANUA-W. J. Berbert
ATTN: CDINS-E

CHIEF of Naval Research
Department of the Navy
Arlington, Ba. 22217
ATTN: CODE 464 Jacob L. Warner
ATTN: CODE 464 Thomas P. Quinn

COMMANDER
Naval Air Systems Command
Headquarters
Washington, D. C. 21360
ATTN: AIR 5381

COMMANDER
Naval Electronics Systems Command
Naval Electronic System CMD HQS
Washington, D. C. 20360
ATTN: NAVALEX 034 T. Barry Hughes
ATTN: PME 106-1 Satellite Comm Project Off
ATTN: John E. Doncarlos
ATTN: PME 117

COMMANDER
Naval Electronics Laboratory Center
San Diego, CA 92152
ATTN: William F. Moler
ATTN: CODE 2200 Verne E. Hildebrand
ATTN: R. Eastman

COMMANDING OFFICER
Naval Intelligence Support CTR
1301 Suitland Road, Bldg. 5
Washington, D. C. 20390
ATTN: Mr. Dubbin Stic 12

DIRECTOR
Naval Research Laboratory
Washington, D. C. 20375
ATTN: HDQ COMM DIR Bruce Wald
ATTN: CODE 5460 Radio Propagation BR
ATTN: CODE 6701 Jack D. Brown
ATTN: CODE 6700 Division Superintendent 25 copies (if unclass)
1 copy (if classified)
ATTN: CODE 6790 Branch Head 150 copies (if unclass)
1 copy (if classified)
ATTN: CODE 7127, Chas. Y. Johnson

COMMANDING OFFICER
Naval Space Surveillance System
Dahlgren, Va. 22448
ATTN: CAPT. J. H. Burton

COMMANDER
Naval Surface Weapons Center
White Oak, Silver Spring, Md. 20910
ATTN: CODE 1224 Navy Nuc Prgms Off
ATTN: CODE 730 Tech. Lib.

DIRECTOR
Strategic Systems Project Office
Navy Department
Washington, D. C. 20376
ATTN: NSP-2141

COMMANDER
ADC/AD
ENT AFB, Co., 80912
ATTN: ADDA

Headquarters
U. S. Army Elect Warfare Lab (ECOM)
White Sands Missile Range, NM 88002
ATTN: E. Butterfield

AF Cambridge Rsch Labs, AFSC
L. G. Hanscom Field
Bedford, Ma 01730
ATTN: LKB Kenneth S. W. Champion
ATTN: OPR James C. Ulwick
ATTN: OPR Hervey P. Gauvin

AF Weapons Laboratory, AFSC
Kirtland AFB, NM 87117
ATTN: John M. Kamm SAS
ATTN: SUL
ATTN: DYT LT Mark A. Fry
ATTN: DYT CAPT Wittwer
ATTN: DYT CAPT Gary Cable

AFTAC
Patrick AFB, Fl. 32925
ATTN: TF MAJ. E. Hines
ATTN: TF/CAPT. Wiley
ATTN: TN

Air Force Avionics Laboratory, AFSC
Wright-Patterson AFB, Oh. 45433
ATTN: AFAL AVWE Wade T. Hunt

Assistant Chief of Staff
Studies and Analysis
Headquarters, U. S. Air Force
Washington, D. C. 20330

Headquarters
Electronics Systems Division (AFSC)
L. G. Hanscom Field
Bedford, Ma. 01730
ATTN: XRE LT. Michaels
ATTN: LTC J. Morin CDEF XRC
ATTN: YSEV

COMMANDER
Foreign Technology Division, AFSC
Wright-Patterson AFB, Oh. 45433
ATTN: TD-BTA LIBRARY

HQ USAF/RD
Washington, D. C. 20330
ATTN: RDQ

COMMANDER
Rome Air Development Center, AFSC
Griffith AFB, N. Y. 13440
ATTN: EMTLD Doc Library

COMMANDER IN CHIEF
Strategic Air Command
Offutt AFB, NB 68113
ATTN: XPFS MAJ. Brian G. Stephan

544IES
Offutt AFB, NB 68113
ATTN: RDPO LT. Alan B. Merrill

Los Alamos Scientific Laboratory
P. O. Box 1663
Los Alamos, NM 87544
ATTN: DOC CON for R. F. Taschek
ATTN: DOC CON for Milton Peek
ATTN: DOC CON for Eric Lindman

Sandia Laboratories
P. O. Box 5800
Albuquerque, NM 87115
ATTN: DOC CON for A. Dean Thronbrough
ATTN: DOC CON for W. D. Brown
ATTN: DOC CON for D. A. Dahlgren, ORG 1722
ATTN: DOC CON for J. P. Martin, ORG 1732

University of California
Lawrence Livermore Laboratory
P. O. Box 808
Livermore, CA 94550
ATTN: Tech Info Dept L-3

Department of Commerce
National Oceanic & Atmospheric Admin.
Environmental Research Laboratories
Boulder, CO 80302
ATTN: Joseph H. Pope
ATTN: C. L. Rufenach

Department of Commerce
Office for Telecommunications
Institute for Telecom Science
Boulder, CO 80302
ATTN: Glenn Falcon
ATTN: G. Reed
ATTN: L. A. Berry
ATTN: William F. Utlaut

Department of Transportation
Transportation Rsch. System Center
Kendall Square
Cambridge, MA 02142
ATTN: TER G. Harowles

NASA
Goddard Space Flight Center
Greenbelt, Md 20771
ATTN: CODE 750 T. Golden

NASA
600 Independence Ave., S. W.
Washington, D. C. 20346
ATTN: M. Dubin

Aerodyne Research, Inc.
Tech/Ops Building
20 South Avenue
Burlington, MA 01803
ATTN: M. Camac
ATTN: F. Bien

Aerospace Corporation
P. O. Box 92957
Los Angeles, CA 90009
ATTN: T. M. Salmi
ATTN: S. P. Bower
ATTN: V. Josephson
ATTN: SMFA for PWW
ATTN: R. Grove
ATTN: R. D. Rawcliffe
ATTN: T. Taylor
ATTN: Harris Mayer
ATTN: D. C. Cartwright

Analytical Systems Corporation
25 Ray Avenue
Burlington, MA 01803
ATTN: Radio Sciences

Avco-Everett Research Laboratory, Inc.
2385 Revere Beach Parkway
Everett, MA 02149
ATTN: Richard M. Patrick

Boeing Company, The
P. O. Box 3707
Seattle, WA 98124
ATTN: D. Murray
ATTN: Glen Keister

Brown Engineering Company, Inc.
Cummings Research Park
Huntsville, AL 35807
ATTN: David Lambert MS 18

California at San Diego, Univ. of
Building 500 Mather Campus
3172 Miramar Road
La Jolla, CA 92037
ATTN: Henry G. Booker

Calspan
P. O. Box 235
Buffalo, N. Y. 14221
ATTN: Romeo A. Deliberis

Computer Sciences Corporation
P. O. Box 530
6565 Arlington Blvd.
Falls Church, VA 22046
ATTN: H. Blank
ATTN: Barbara F. Adams

Comsat Laboratories
P. O. Box 115
Clarksburg, Md. 20734
ATTN: R. R. Taur

Cornell University
Department of Electrical Engineering
Ithaca, N. Y. 14850
ATTN: D. T. Farley, Jr.

ESL, Inc.
495 Java Drive
Sunnyvale, CA 93102
ATTN: J. Roberts
ATTN: V. L. Mower
ATTN: James Marshall
ATTN: R. K. Stevens

General Electric Company
Tempo-Center for Advanced Studies
816 State Street
Santa Barbara, CA 93102
ATTN: Don Chandler
ATTN: DASIAC
ATTN: Tim Stephens

General Electric Company
P. O. Box 1122
Syracuse, N. Y. 13201
ATTN: F. A. Reibert

General Research Corporation
P. O. Box 3587
Santa Barbara, CA 93105
ATTN: John Ise, Jr.

Geophysical Institute
University of Alaska
Fairbanks, AK 99701
ATTN: Technical Library
ATTN: Neil Brown
ATTN: T. N. Davis

GTE Sylvania, Inc.
189 B Street
Needham Heights, MA 02194
ATTN: Marshall Cross

HRB-SINGER, Inc.
Science Park, Science Park Road
P. O. Box 60
State College, PA 16801
ATTN: Larry Feathers

Honeywell Incorporated
Radiation Center
2 Forbes Road
Lexington, MA 02173
ATTN: W. Williamson

Illinois, University of
Department of Electrical Engineering
Urbana, IL 61801
ATTN: K. C. Yeh

Institute for Defense Analyses
400 Army-Navy Drive
Arlington, VA 22202
ATTN: Ernest Bauer
ATTN: Hans Wolfhard
ATTN: J. M. Aein
ATTN: Joel Bengston

Intl Tel & Telegraph Corporation
500 Washington Avenue
Nutley, N. J. 07110
ATTN: Technical Library

ITT Electro-Physics Laboratories, Inc.
9140 Old Annapolis Road
Columbus, Md. 21043
ATTN: John M. Kelso

Johns Hopkins University
Applied Physics Laboratory
8621 Georgia Avenue
Silver Spring, MD 20910
ATTN: Document Librarian

Lockheed Missiles & Space Co., Inc.
P. O. Box 504
Sunnyvale, CA 94088
ATTN: Dept. 60-12

Lockheed Missiles and Space Company
3251 Hanover Street
Palo Alto, CA 94304
ATTN: Billy M. McCormac, Dept 52-14
ATTN: Martin Walt, Dept 52-10
ATTN: Richard G. Johnson, Dept 52-12
ATTN: JOHN CLADIS

MIT Lincoln Laboratory
P. O. Box 73
Lexington, MA 02173
ATTN: Mr. Walden, X113
ATTN: D. Clark
ATTN: James H. Pannell, L-246
ATTN: Lib A-082 for David M. Towle

Martin Marietta Corporation
Denver Distribution
P. O. Box 179
Denver, CO 80201
ATTN: Special Projects Program 248

Maxwell Laboratories, Inc.
9244 Balboa Avenue
San Diego, CA 92123
ATTN: A. J. Shannon
ATTN: V. Fargo
ATTN: A. N. Rostocker

McDonnell Douglas Corporation
5301 Bolsa Avenue
Huntington Beach, CA 92657
ATTN: J. Moule
ATTN: N. Harris

Mission Research Corporation
735 State Street
Santa Barbara, CA 93101
ATTN: R. Hendrick
ATTN: Conrad L. Longmire
ATTN: Ralph Kilb
ATTN: R. E. Rosenthal
ATTN: R. Bogusch
ATTN: David Sowle
ATTN: M. Scheibe
ATTN: P. Fischer

Mitre Corporation, The
Route 62 and Middlesex Turnpike
P. O. Box 208
Bedford, MA 01730
ATTN: Chief Scientist W. Sen
ATTN: S. A. Morin M/S
ATTN: C. Harding

North Carolina State Univ At Raleigh
Raleigh, N. C. 27507
ATTN: SEC Officer for Walter A. Flood

Pacific-Sierra Research Corp.
1456 Cloverfield Blvd.
Santa Monica, CA 90404
ATTN: E. C. Field, Jr.

Philco-Ford Corporation
Western Development Laboratories Div
3939 Fabian Way
Palo Alto, CA 94303
ATTN: J. T. Mattingley MS X22

Photometrics, Inc.
442 Marrett Road
Lexington, MA 02173
ATTN: Irving J. Kofsky

Mitre Corporation, The
Westgate Research Park
1820 Dolley Madison Blvd.
McLean, VA 22101
ATTN: Allen Schneider

Physical Dynamics, Inc.
P. O. Box 1069
Berkeley, CA 94701
ATTN: Joseph B. Workman

Physical Sciences, Inc.
607 North Avenue, Door 18
Wakefield, MA 01880
ATTN: Kurt Wray

R & D Associates
P. O. Box 3580
Santa Monica, CA 90403
ATTN: Robert E. Lelevier
ATTN: Forest Gilmore
ATTN: Richard Latter
ATTN: William B. Wright, Jr.

R & D Associates
1815 N. Ft. Myer Drive
11th Floor
Arlington, VA 2209
ATTN: Herbert J. Mitchell

Rand Corporation, The
1700 Main Street
Santa Monica, CA 90406
ATTN: Cullen Crain

Science Applications, Inc.
P. O. Box 2351
La Jolla, CA 92038
ATTN: Daniel A. Hamlin
ATTN: D. Sachs
ATTN: E. A. Straker

Space Data Corporation
1331 South 26th Street
Phoenix, AZ 85034
ATTN: Edward F. Allen

Stanford Research Institute
333 Ravenswood Avenue
Menlo Park, CA 94025
ATTN: M. Baron
ATTN: L. L. Cobb
ATTN: Walter G. Chestnut
ATTN: David A. Johnson
ATTN: Charles L. Rino
ATTN: E. J. Fremouw
ATTN: Ray L. Leadabrand
ATTN: Donald Neilson

Stanford Research Institute
306 Wynn Drive, N. W.
Huntsville, AL 35805
ATTN: Dale H. Davis

Technology International Corporation
75 Wiggins Avenue
Bedford, MA 01730
ATTN: W. P. Boquist

TRW Systems Group
One Space Park
Redondo Beach, CA 90278
ATTN: P. H. Katsos
ATTN: J. W. Lowery

Utah State University
Logan, UT 84321
ATTN: C. Wyatt
ATTN: D. Burt
ATTN: Kay Baker
ATTN: Doran Baker

Visidyne, Inc.
19 Third Avenue
North West Industrial Park
Burlington, MA 01803
ATTN: William Reidy
ATTN: Oscar Manley
ATTN: J. W. Carpenter